Supporting Information

Bis-isatin based polymers with tunable energy levels for organic field-effect transistor applications

Wei Yang,[a] Mingxiang Sun,[b] Yue Wang,[c] Hui Yan,[c] Guobing Zhang*[b] and Qing Zhang*[a]

[a]*Shanghai Key Laboratory of Electrical Insulation and Thermal Aging, School of Chemistry and Chemical Engineering, Shanghai Jiaotong University, 800 Dongchuan Road, Shanghai, China;* orcid.org/0000-0001-5934-8384; *E-mail: qz14@sjtu.edu.cn (Q. Zhang).*

[b]*Special Display and Imaging Technology Innovation Center of Anhui Province, State Key Laboratory of Advanced Display Technology, Academy of Opto-Electronic Technology, Hefei University of Technology, Hefei, China;* orcid.org/0000-0001-6053-2015*; E-mail: gbzhang@hfut.edu.cn (G. Zhang)*

[c]*School of Pharmacy, Liaocheng Unversity, Liaocheng*, China; orcid.org/0000-0002-9843-0601.

1. NMR and Mass Spectra of compounds

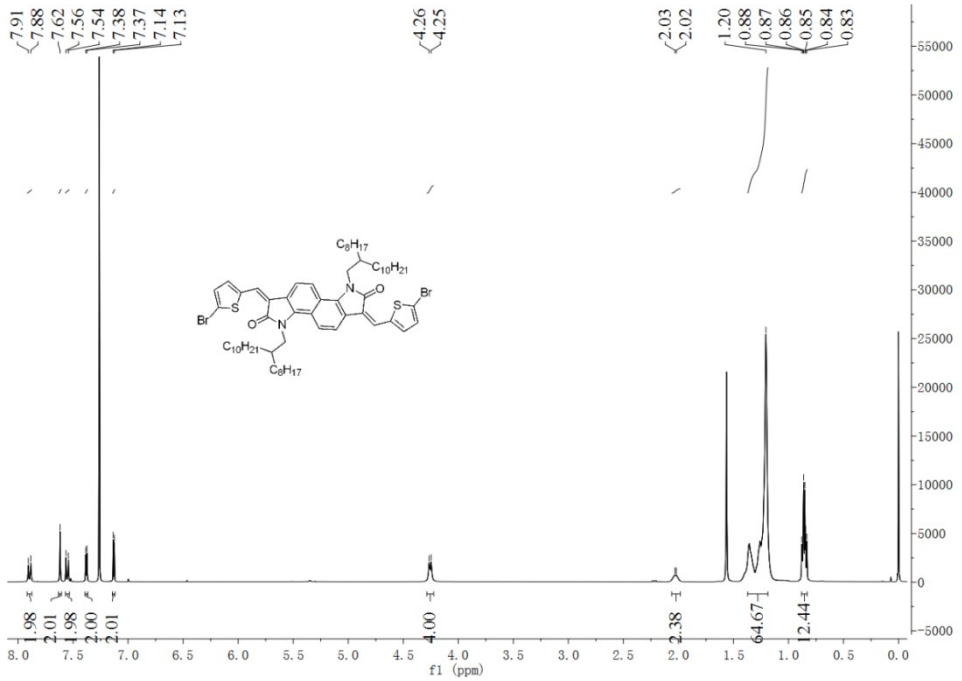

Figure S1. ^{1}H NMR spectrum of **BTEI** in $CDCl_3$

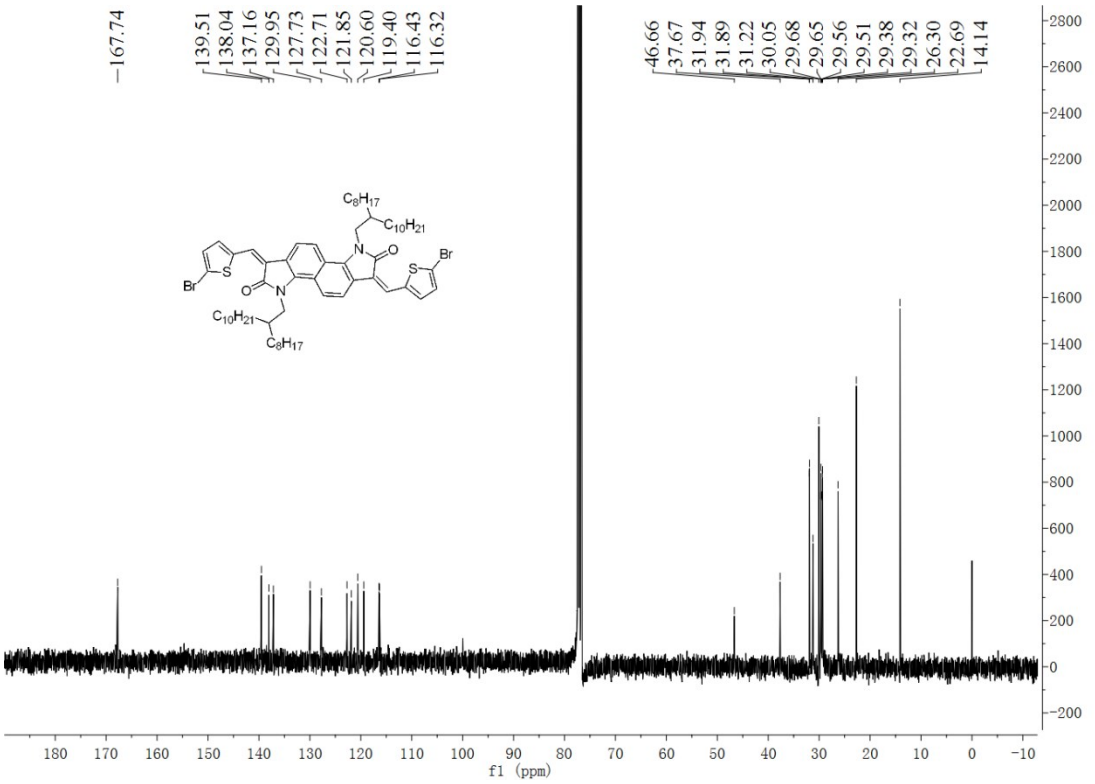

Figure S2. ^{13}C NMR spectrum of **BTEI** in $CDCl_3$

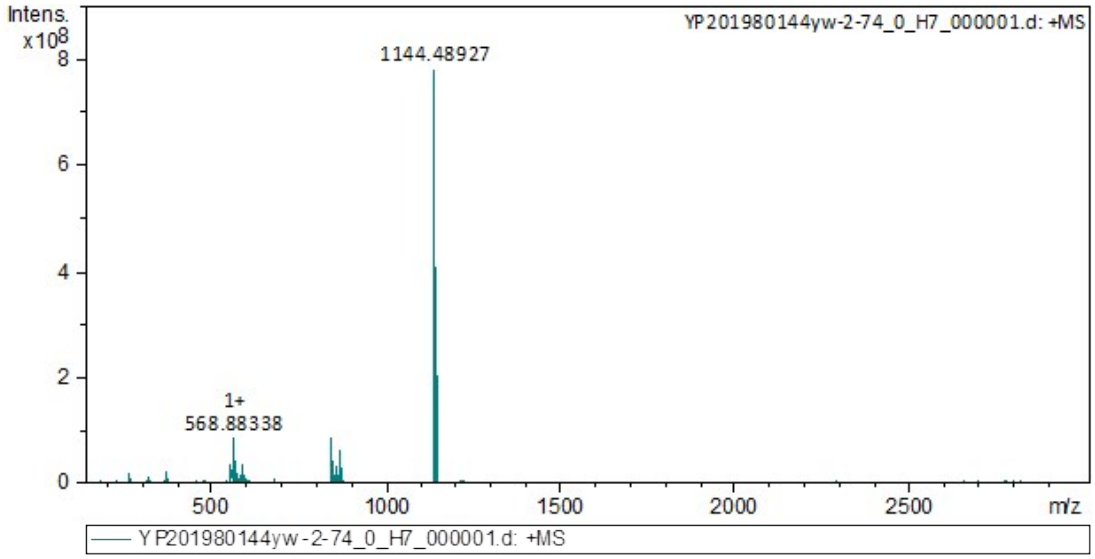

Figure S3. High-resolution MALDI-TOF spectrum of **BTEI**.

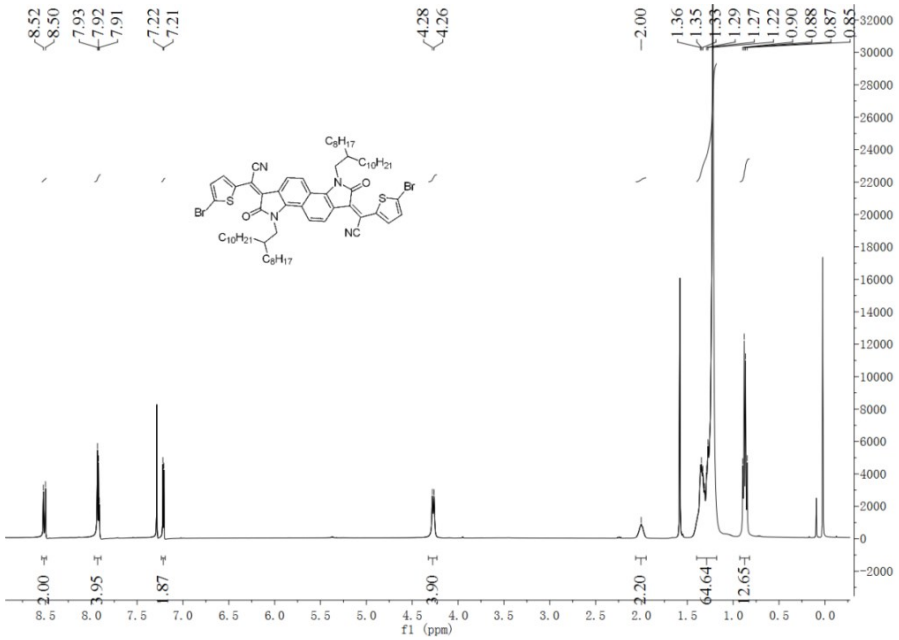

Figure S4. ^{1}H NMR spectrum of **BTEI(CN)** in $CDCl_3$

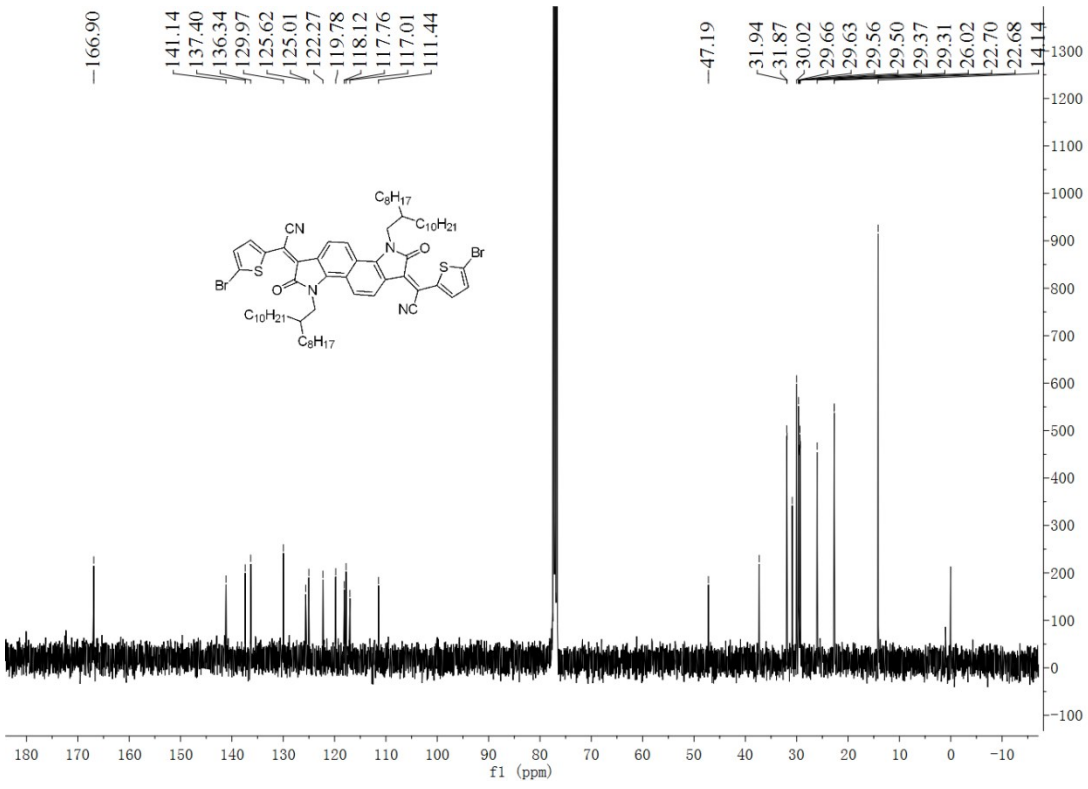

Figure S5. ^{13}C NMR spectrum of **BTEI(CN)** in $CDCl_3$

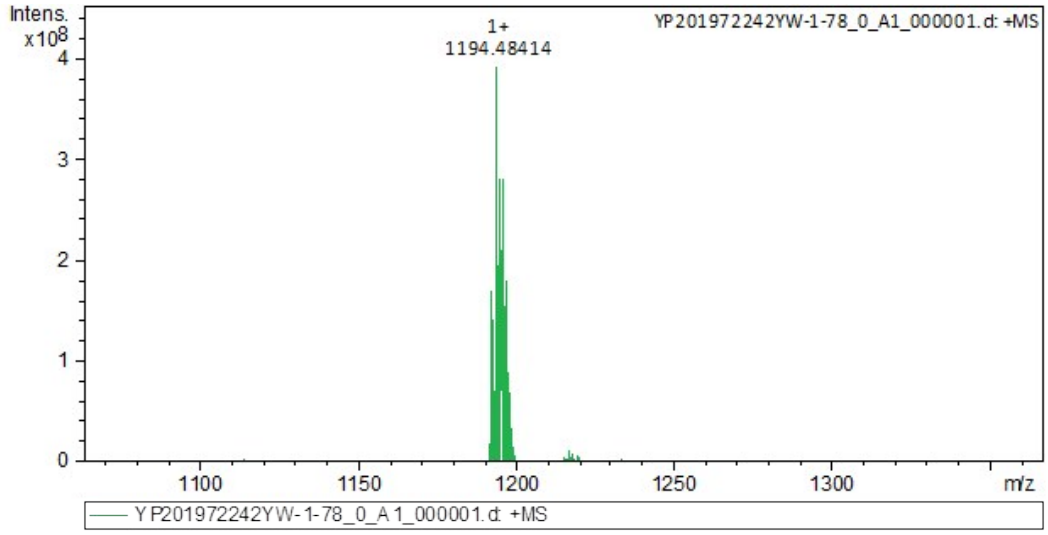

Figure S6. High-resolution MALDI-TOF spectra of **BTEI(CN)**.

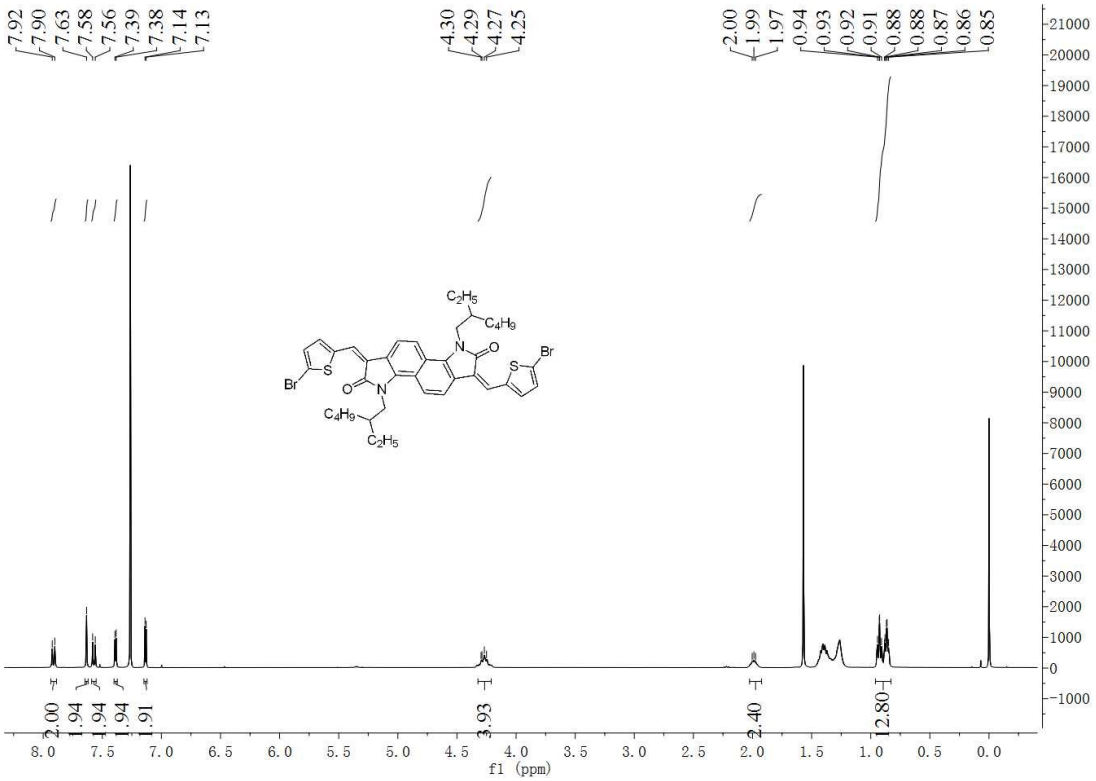

Figure S7. ^{1}H NMR spectrum of **BTEI-C8** in $CDCl_3$

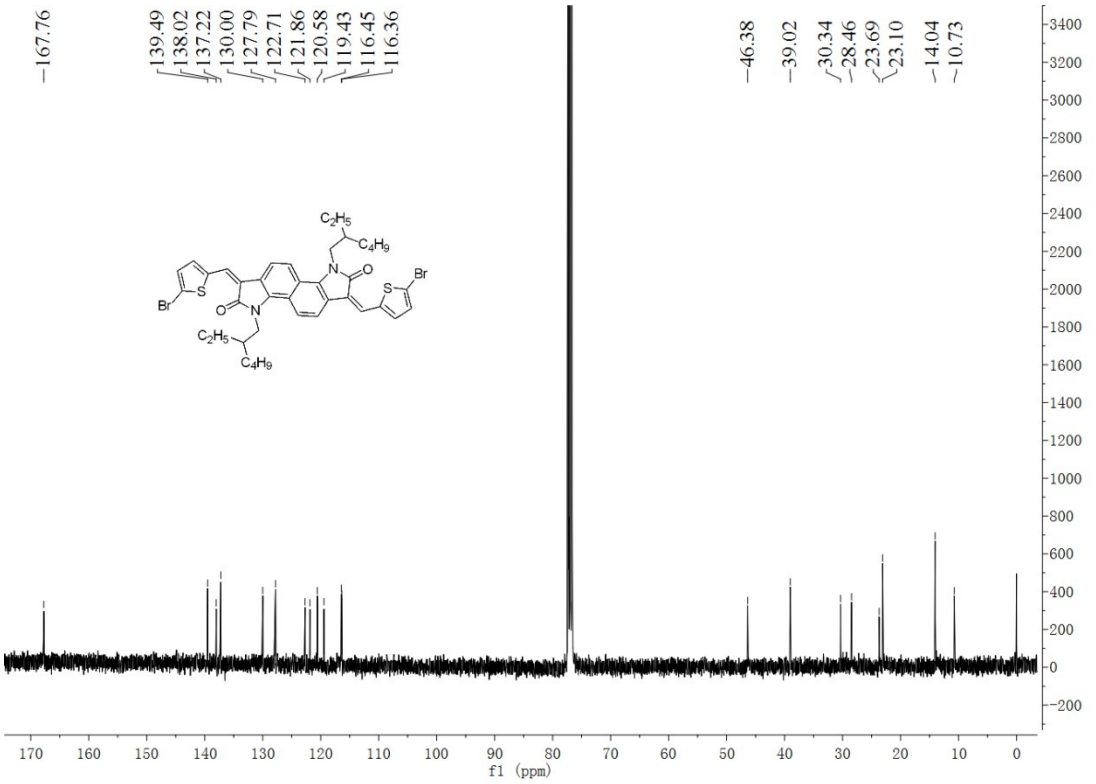

Figure S8. ^{1}C NMR spectrum of **BTEI-C8** in $CDCl_3$

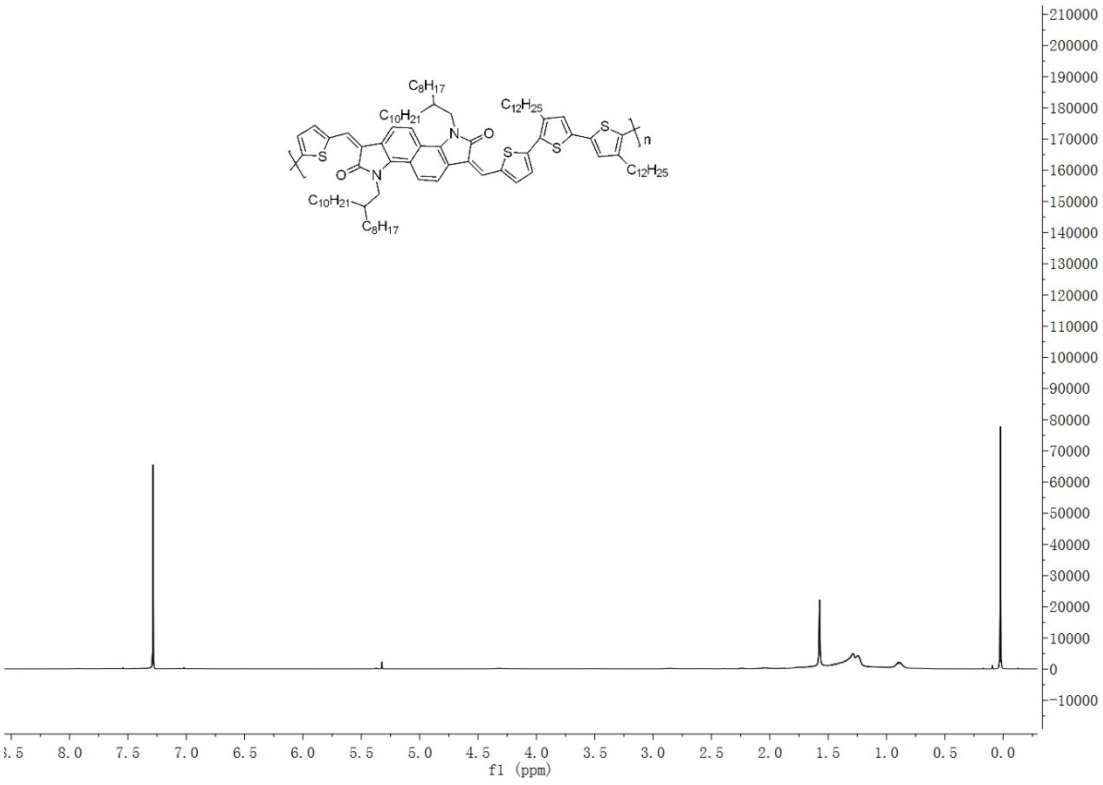

Figure S9. ^{1}H NMR spectrum of **P1** in $CDCl_3$

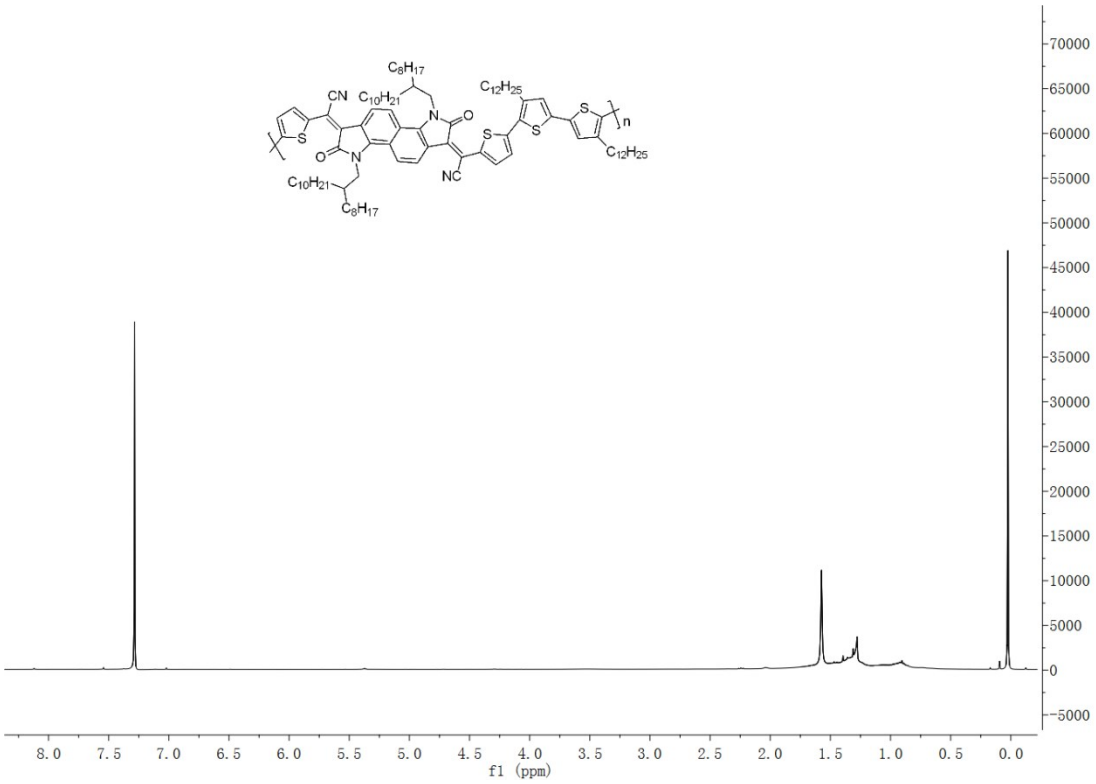

Figure S10. ^{1}H NMR spectrum of **P2** in $CDCl_3$

2. Crystallographic results

Table S1. Crystal data and structure refinement for **BTEI**.

Empirical formula	$C_{40}\ H_{34}\ Br_2\ N_2\ O_2\ S_2$
Formula weight	798.63
Temperature	173(2) K
Wavelength	1.54178 A
Crystal system, space group	Triclinic, P-1
Unit cell dimensions	a = 7.845(3) A alpha = 73.92(3) deg
	b = 10.433(2) A beta = 89.21(3) deg
	c = 15.690(7) A gamma = 70.37(2) deg
Volume	1157.7(8) A^3
Z, Calculated density	1, 1.146 Mg/m^3
Absorption coefficient	3.292 mm^-1
F(000)	406
Crystal size	0.200 x 0.180 x 0.150 mm
Theta range for data	4.701 to 68.342 deg

collection	
Limiting indices	-9<=h<=9, -12<=k<=12, -18<=l<=18
Reflections collected / unique	15838 / 4228 [R(int) = 0.0342]
Completeness to theta	67.679 99.6 %
Refinement method	Full-matrix least-squares on F^2
Data / restraints / parameters	4228 / 1 / 218
Goodness-of-fit on F^2	1.434
Final R indices [I>2sigma(I)]	R1 = 0.0991, wR2 = 0.3312
R indices (all data)	R1 = 0.1137, wR2 = 0.3571
Extinction coefficient	n/a
Largest diff. peak and hole	0.616 and -0.390 e.A^-3

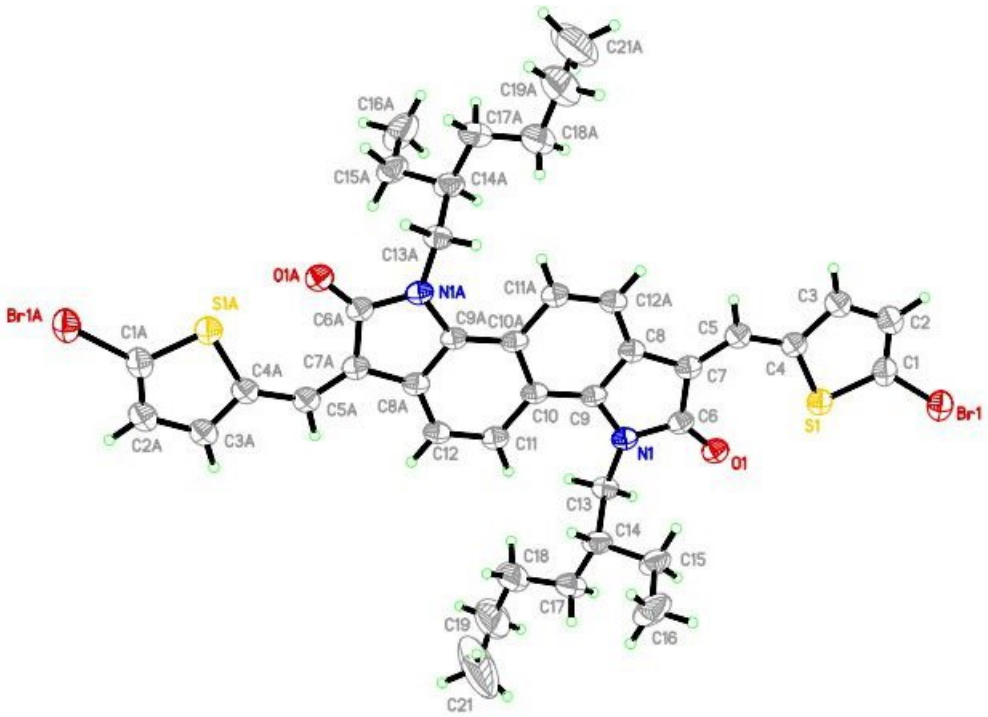

Figure S11. Single crystal structures of **BTEI**

Table S2. Selected Torsion angles (˚) for Compound **BTEI**

Bond type	Torsion angles (˚)
S(1)-C(4)-C(5)-C(7)	0.2
N(1)-C(9)-C(10)-C(11)	0.9
O(1)-C(6)-C(7)-C(5)	-1.6

3. Thermal Analyses of Polymer

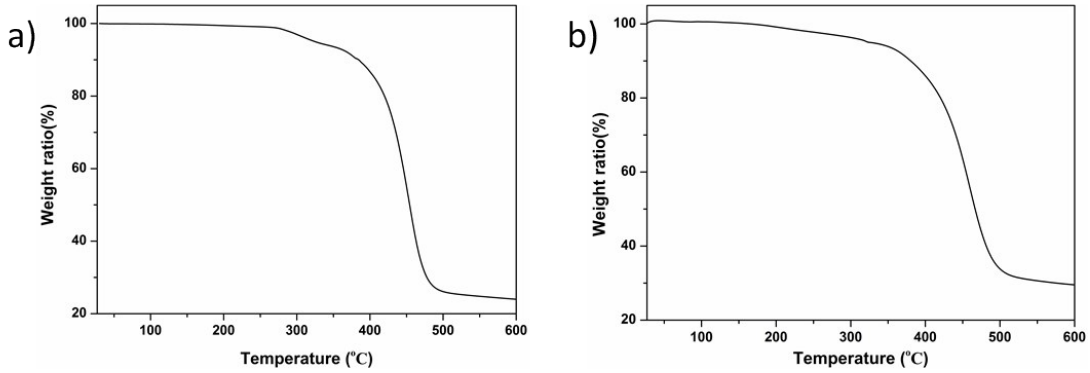

Figure S12. Thermogravimetric analysis (TGA) analysis of (a) **P1** and (b) **P2**

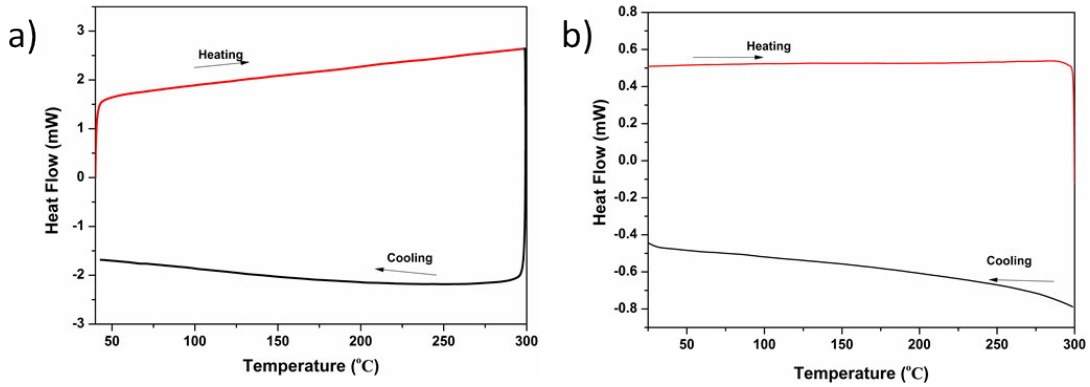

Figure S13. Differential scanning calorimetry (DSC) analysis of (a) **P1** and (b) **P2**

4. OFET device performance of polymers.

Table S3. OFET device performance of **P1** and **P2** polymers

Compd	$T_{annealing}$ (°C)	$\mu_{h,max}(\mu_{h,avg})$ ($cm^2V^{-1}s^{-1}$) [a]	V_{th}(V)	I_{on}/I_{off}	$\mu_{e,max}(\mu_{e,avg})$ ($cm^2V^{-1}s^{-1}$) [b]	V_{te}(V)	I_{on}/I_{off}
P1	N/A	0.029(0.027)	-3.2	10^4			
	180	0.230(0.210)	-2.7	10^6			
	210	0.270(0.240)	-3.7	10^6			
P2	N/A	0.051(0.047)	10.1	10^3			
	180	0.068(0.064)	9.3	10^3	0.023(0.020)	23.6	10^6
	210	0.094(0.089)	13.7	10^3	0.024(0.020)	31.1	10^6

[a]Device fabricated in ambient conditions. [b]Devices fabricated in glovebox.